

Analytic results for Gaussian wave packets in four model systems:

I. Visualization of the kinetic energy

R. W. Robinett and L. C. Bassett

Department of Physics

The Pennsylvania State University

University Park, PA 16802 USA

(Dated: November 26, 2024)

Abstract

Using Gaussian wave packet solutions, we examine how the kinetic energy is distributed in time-dependent solutions of the Schrödinger equation corresponding to the cases of a free particle, a particle undergoing uniform acceleration, a particle in a harmonic oscillator potential, and a system corresponding to an unstable equilibrium. We find, for specific choices of initial parameters, that as much as 90% of the kinetic energy can be localized (at least conceptually) in the ‘front half’ of such Gaussian wave packets, and we visualize these effects.

I. INTRODUCTION

The study of time-dependent solutions of the Schrödinger equation for initial wave packets of Gaussian form has a long history, dating back to the earliest days of the development of quantum theory. Schrödinger himself [1] and others [2] - [4] used such solutions to discuss the connections between the quantum and classical formulations of mechanics and found explicit wave packet solutions to many of the standard problems of classical mechanics, including the free-particle, case of uniform acceleration, the harmonic oscillator, and the particle in a uniform magnetic field. These examples first appeared in a number of textbooks [5] - [7] less than a decade later.

In contrast, many treatments of introductory quantum mechanics today focus almost exclusively on time-independent, energy eigenstate (or stationary state) solutions of the Schrödinger equation, although a large number of texts do include the explicit construction of a time-dependent Gaussian wave packet solution for the free-particle case. This easily obtained, analytic result (seemingly first obtained by Darwin [3]) illustrates, in a closed form solution, many of the notions central to wave packet spreading and the essentially classical time-development of the expectation value as $\langle x \rangle_t = \langle p \rangle_0 t / m + \langle x \rangle_0$. In many modern software packages, these solutions are also visualized, helping to illustrate the correlated time-development of the real and imaginary parts, and especially their phase relationships, often using a popular color-coding scheme [8], [9], [10].

An example of a static image representing such time-development is shown in Fig. 1. One can easily note the non-symmetric pattern of the ‘wiggleness’ apparent for $t > 0$ in both the real (dotted) and imaginary (dashed) parts of $\psi(x, t)$, which, as we will argue below, can be used as a qualitative measure of the local kinetic energy. The faster (higher momentum, and hence ‘wigglier’) components are more obviously associated with the ‘front end’ of the spreading wave packet, while the ‘back end’ exhibits much less rapid spatial variation, consistent with the slower (low momentum) components trailing behind.

In this note, we attempt to extend and amplify upon this type of intuitive observation and try to answer such questions as *Where is the kinetic energy localized in a wave packet?* To this end, we begin with the familiar observation that the expectation value of the kinetic energy operator in any time-dependent position-space state, $\psi(x, t)$, can be written, using a

simple integration-by-parts (or IBP) argument, in the form

$$\begin{aligned} \langle \hat{T} \rangle &= \frac{1}{2m} \langle \hat{p}^2 \rangle = -\frac{\hbar^2}{2m} \int_{-\infty}^{+\infty} dx \psi^*(x, t) \frac{\partial^2 \psi(x, t)}{\partial x^2} \\ &\stackrel{IBP}{=} -\frac{\hbar^2}{2m} \left(\psi^*(x, t) \frac{\partial \psi(x, t)}{\partial x} \right)_{-\infty}^{+\infty} \\ &\quad + \frac{\hbar^2}{2m} \int_{-\infty}^{+\infty} dx \frac{\partial \psi^*(x, t)}{\partial x} \frac{\partial \psi(x, t)}{\partial x} \end{aligned} \quad (1)$$

or

$$\langle \hat{T} \rangle = \frac{\hbar^2}{2m} \int_{-\infty}^{+\infty} dx \left| \frac{\partial \psi(x, t)}{\partial x} \right|^2 \quad (2)$$

where the ‘boundary terms’ (involving ψ and $\partial\psi/\partial x$ at $\pm\infty$) are assumed to vanish for any appropriately localized solution.

This global identification suggests that we define a local *kinetic energy density*, $\mathcal{T}(x, t)$, via

$$\mathcal{T}(x, t) \equiv \frac{\hbar^2}{2m} \left| \frac{\partial \psi(x, t)}{\partial x} \right|^2 \quad \text{where} \quad \langle \hat{T} \rangle_t = \int_{-\infty}^{+\infty} \mathcal{T}(x, t) dx \equiv T(t). \quad (3)$$

This quantity, which is clearly locally real and positive-definite, can then be used to quantify the distribution of kinetic energy, and how it changes with time, for any time-dependent solution of the Schrödinger equation. For Gaussian solutions, we will be able to perform many of the desired integrals in closed form, leading to explicit analytic results for such related quantities as

$$T^{(+)}(t) \equiv \int_{\langle x \rangle_t}^{+\infty} \mathcal{T}(x, t) dx \quad \text{and} \quad T^{(-)}(t) \equiv \int_{-\infty}^{\langle x \rangle_t} \mathcal{T}(x, t) dx \quad (4)$$

where the expectation value $\langle x \rangle_t$ serves to define the ‘center’ of the wave packet. These quantities can be respectively associated with the kinetic energy in the ‘right’ (or ‘front’, at least for packets moving generally to the right) half and the ‘left’ (or ‘back’) half of the wave packet.

In what follows, we will present several explicit closed-form examples of the calculation of $T^{(\pm)}(t)$ for Gaussian wave packet solutions, starting in Sec. II with free-particle wave packets for a standard Gaussian momentum distribution, while in Sec. III we illustrate similar results for Gaussian solutions to the problem of a particle undergoing uniform acceleration, working initially in momentum-space. In Sec. IV we use standard propagator techniques to examine

Gaussian wave packet solutions for the harmonic oscillator problem in this context, while in Sec. V we extend these results to the case of an ‘inverted oscillator’, corresponding to a particle in unstable equilibrium.

II. FREE-PARTICLE GAUSSIAN WAVE PACKETS

The time-dependent Schrödinger equation for the one-dimensional free particle case can be written, and easily solved, in either position- or momentum-space in the equivalent forms

$$-\frac{\hbar^2}{2m} \frac{\partial^2 \psi(x, t)}{\partial x^2} = i\hbar \frac{\partial \psi(x, t)}{\partial t} \quad \text{or} \quad \frac{p^2}{2m} \phi(p, t) = i\hbar \frac{\partial \phi(p, t)}{\partial t}. \quad (5)$$

Since we will find the momentum-space approach more useful in Sec. III for the case of uniform acceleration, we will also use that approach here and write

$$\phi(p, t) = \phi_0(p) e^{-ip^2 t / 2m\hbar} \quad (6)$$

where $\phi(p, 0) = \phi_0(p)$ is the initial momentum distribution. Using this very general form, and the appropriate operator form of $\hat{x} = i\hbar(\partial/\partial p)$, we recall that

$$\begin{aligned} \langle \hat{x} \rangle_t &= \int_{-\infty}^{+\infty} \phi^*(p, t) \left(i\hbar \frac{\partial}{\partial p} \right) \phi(p, t) dp \\ &= \int_{-\infty}^{+\infty} \phi_0^*(p) \hat{x} \phi_0(p) dp + \frac{t}{m} \int_{-\infty}^{+\infty} p |\phi_0(p)|^2 dp \\ &= \langle \hat{x} \rangle_0 + \frac{\langle p \rangle_0 t}{m}. \end{aligned} \quad (7)$$

The position-space solution can be written, of course, using the Fourier transform as

$$\psi(x, t) = \frac{1}{\sqrt{2\pi\hbar}} \int_{-\infty}^{+\infty} e^{ipx/\hbar} \phi(p, t) dp. \quad (8)$$

The standard initial Gaussian momentum-space distribution, which gives arbitrary initial momentum (p_0) and position (x_0) values, can be written in the form

$$\phi(p, 0) = \phi_0(p) = \sqrt{\frac{\alpha}{\sqrt{\pi}}} e^{-\alpha^2(p-p_0)^2/2} e^{-ipx_0/\hbar} \quad (9)$$

which gives

$$\langle p \rangle_t = p_0, \quad \langle p^2 \rangle_t = p_0^2 + \frac{1}{2\alpha^2}, \quad \text{and} \quad \Delta p_t = \Delta p_0 = \frac{1}{\alpha\sqrt{2}}. \quad (10)$$

The explicit form of the position-space wave function is given by the Gaussian integral

$$\psi(x, t) = \frac{1}{\sqrt{2\pi\hbar}} \sqrt{\frac{\alpha}{\sqrt{\pi}}} \int_{-\infty}^{+\infty} e^{ip(x-x_0)/\hbar} e^{-\alpha^2(p-p_0)^2/2} e^{-ip^2t/2m\hbar} dp \quad (11)$$

which can be evaluated in closed form (using the change of variables $q \equiv p - p_0$ and standard integrals) to obtain

$$\psi(x, t) = \frac{1}{\sqrt{\sqrt{\pi}\alpha\hbar(1+it/t_0)}} e^{ip_0(x-x_0)/\hbar} e^{-ip_0^2t/2m\hbar} e^{-(x-x_0-p_0t/m)^2/2(\alpha\hbar)^2(1+it/t_0)} \quad (12)$$

where $t_0 \equiv m\hbar\alpha^2$. (This result is sometimes attributed to Darwin [3].) The corresponding probability density is easily shown to be

$$P(x, t) = |\psi(x, t)|^2 = \frac{1}{\sqrt{\pi}\beta_t} e^{-(x-x(t))^2/\beta_t^2} \quad (13)$$

where

$$x(t) \equiv x_0 + p_0t/m \quad \text{and} \quad \beta_t \equiv \alpha\hbar\sqrt{1+t^2/t_0^2} \quad (14)$$

and the time-dependent expectation values of position are

$$\langle x \rangle_t = x(t) = x_0 + p_0t/m, \quad \langle x^2 \rangle_t = (x(t))^2 + \frac{\beta_t^2}{2}, \quad \text{and} \quad \Delta x_t = \frac{\beta_t}{\sqrt{2}}, \quad (15)$$

all of which are familiar results.

Turning now to the kinetic energy distribution defined in Eqn. (3), we find that the required spatial derivative is given by

$$\frac{\partial\psi(x, t)}{\partial x} = \left(\frac{ip_0}{\hbar} - \frac{(x-x(t))}{(\alpha\hbar)^2(1+it/t_0)} \right) \psi(x, t). \quad (16)$$

The kinetic energy density can therefore be written in the form

$$\mathcal{T}(x, t) = \frac{1}{2m} \left(p_0^2 + \left[\frac{2(x-x(t))p_0}{\alpha^2\hbar} \right] \left[\frac{t/t_0}{(1+t^2/t_0^2)} \right] + \frac{(x-x(t))^2}{(\alpha^2\hbar)^2(1+t^2/t_0^2)} \right) |\psi(x, t)|^2. \quad (17)$$

The expectation value of the kinetic energy is correctly given by

$$T(t) = \int_{-\infty}^{+\infty} \mathcal{T}(x, t) dx = \frac{1}{2m} \left(p_0^2 + \frac{1}{2\alpha^2} \right) \quad (18)$$

and receives non-zero contributions from the first and last terms in brackets in Eqn. (17), since the middle term vanishes (when integrated over all space) for symmetry reasons. On the other hand, the individual values of $T^{(\pm)}(t)$ in Eqn. (4) can also be evaluated giving

$$T^{(\pm)}(t) = \frac{1}{2m} \left(\frac{1}{2} \right) \left(p_0^2 \pm \left(\frac{2p_0}{\alpha\sqrt{\pi}} \right) \frac{t/t_0}{\sqrt{1+t^2/t_0^2}} + \frac{1}{2\alpha^2} \right) \quad (19)$$

both of which are easily seen to be positive definite, as they must, due to the non-negativity of $\mathcal{T}(x, t)$. The time-dependent fractions of the total kinetic energy contained in the (+)/(-) (right/left) halves of this archetypical wave packet are given by

$$R^{(\pm)}(t) \equiv \frac{T^{(\pm)}(t)}{T^{(+)}(t) + T^{(-)}(t)} = \frac{1}{2} \pm \left(\frac{2}{\sqrt{\pi}} \right) \left(\frac{(p_0\alpha)}{(2(p_0\alpha)^2 + 1)} \right) \frac{t/t_0}{\sqrt{1 + t^2/t_0^2}} \quad (20)$$

which will clearly increase/decrease monotonically as $t/t_0 \rightarrow \infty$. The limiting values are then

$$R^{(\pm)}(t/t_0 \rightarrow \infty) = \frac{1}{2} \pm \left(\frac{2}{\sqrt{\pi}} \right) \left(\frac{(p_0\alpha)}{(2(p_0\alpha)^2 + 1)} \right) \quad (21)$$

which have the extremal values

$$R_{max}^{(+)}(t/t_0 \rightarrow \infty) = \frac{1}{2} + \frac{1}{\sqrt{2\pi}} \approx 0.9 \quad \text{and} \quad R_{min}^{(-)}(t/t_0 \rightarrow \infty) = \frac{1}{2} - \frac{1}{\sqrt{2\pi}} \approx 0.1 \quad (22)$$

which occur when

$$p_0\alpha = \frac{1}{\sqrt{2}} \quad \text{or} \quad p_0 = \frac{1}{\alpha\sqrt{2}} = \Delta p_0. \quad (23)$$

Thus, as much as 90% of the total kinetic energy of this Gaussian wave packet solution can be in the ‘front half’ of the wave at long times (i.e. those for which $t \gg t_0$.)

To illustrate this effect, we plot in the left column of Fig. 2, the modulus ($|\psi(x, t)|$, solid), and real (dotted) and imaginary (dashed) parts of a typical solution corresponding to $p_0 = 0$ (top), $p_0 = \Delta p_0$ (the extremal value, middle), and $p_0 = 4\Delta p_0$ (bottom) for long times ($t = 10t_0$). The values are plotted in terms of the variable $x(t) = x_0 + p_0 t/m$ for easier comparison. For the $p_0 = 0$ case, it is clear that the larger momentum components (in magnitude) spread faster, but uniformly, in the opposite $+x$ and $-x$ directions, giving equal ‘wiggleness’ on each side, while for large values of p_0 , the total kinetic energy is clearly increased (many more ‘wiggles’ everywhere), but the amount on each side of the expectation value peak at $\langle x \rangle_t$ is roughly the same. For the extremal value of $p_0 = \Delta p_0$, there is the clearest distinction between the ‘front’ and ‘back’ halves, as the magnitudes of the momentum components in the ‘back’ half are at a minimum, resulting in the greatest separation between the kinetic energy in the two halves.

We can also compare the distribution of probability, described as usual by $P(x, t) \equiv |\psi(x, t)|^2$, to how the kinetic energy is localized. The kinetic energy density, $\mathcal{T}(x, t)$, can be

scaled to the total (and possibly time-dependent) value of $T(t)$ via

$$S(x, t) \equiv \frac{\mathcal{T}(x, t)}{T(t)} \quad \text{which satisfies} \quad \int_{-\infty}^{+\infty} S(x, t) dx = 1 \quad (24)$$

and so is normalized in the same way as the probability density. We plot both $P(x, t)$ (solid curve) and $S(x, t)$ (dot-dashed curve) in the right hand column of Fig. 2 for the same three cases considered above and we note how the shape of $S(x, t)$ is correlated with the obvious ‘wiggleness’ shown in the real and imaginary parts of $\psi(x, t)$.

III. UNIFORM ACCELERATION

The problem of a particle under the influence of a constant force is a staple in classical mechanics, and was considered early in the history of quantum mechanics [5], but is less often discussed in introductory treatments of the subject, especially in terms of time-dependent solutions. For that reason, we briefly review the most straightforward momentum-space approach to this problem. In this case, where the potential is given by $V(x) = -Fx$, we can write the time-dependent Schrödinger equation in momentum-space as

$$\frac{p^2}{2m}\phi(p, t) - F \cdot \left[i\hbar \frac{\partial}{\partial p} \right] \phi(p, t) = i\hbar \frac{\partial \phi(p, t)}{\partial t} \quad (25)$$

or

$$i\hbar \left(F \frac{\partial \phi(p, t)}{\partial p} + \frac{\partial \phi(p, t)}{\partial t} \right) = \frac{p^2}{2m} \phi(p, t). \quad (26)$$

We note that the simple combination of derivatives guarantees that a function of the form $\Phi(p - Ft)$ will make the left-hand side vanish, so we assume a solution of the form $\phi(p, t) = \Phi(p - Ft)\tilde{\phi}(p)$, with $\Phi(p)$ arbitrary and $\tilde{\phi}(p)$ to be determined. Using this form, Eqn. (26) reduces to

$$\frac{\partial \tilde{\phi}(p)}{\partial p} = -\frac{ip^2}{2m\hbar F} \tilde{\phi}(p) \quad (27)$$

with the solution

$$\tilde{\phi}(p) = e^{-ip^3/6mF\hbar}. \quad (28)$$

We can then write the general solution as

$$\phi(p, t) = \Phi(p - Ft)e^{-ip^3/6mF\hbar} \quad (29)$$

or, using the arbitrariness of $\Phi(p)$, as

$$\phi(p, t) = \phi_0(p - Ft) e^{i((p - Ft)^3 - p^3)/6mF\hbar} \quad (30)$$

where now $\phi_0(p)$ is some initial momentum distribution since $\phi(p, 0) = \phi_0(p)$. Note that because the p^3 terms cancel in the exponential, we will be able to explicitly integrate Gaussian type initial momentum-space waveforms.

For any general initial $\phi_0(p)$ we now have the time-dependent expectation values

$$\langle p \rangle_t = \langle p \rangle_0 + Ft \quad (31)$$

$$\langle p^2 \rangle_t = \langle p^2 \rangle_0 + 2\langle p \rangle_0 Ft + (Ft)^2 \quad (32)$$

$$\langle \hat{x} \rangle_t = \langle \hat{x} \rangle_0 + \frac{\langle p \rangle_0 t}{m} + \frac{Ft^2}{2m} \quad (33)$$

which also give the expectation value

$$\left\langle \frac{p^2}{2m} + V(x) \right\rangle = \frac{\langle p^2 \rangle_0}{2m} - F\langle \hat{x} \rangle_0 \quad (34)$$

which, in turn, also agrees with a similar calculation of $\langle \hat{E} \rangle_t$ using $\hat{E} = i\hbar(\partial/\partial t)$, all of which are consistent with a particle undergoing uniform acceleration.

Using the standard initial Gaussian momentum-space wavefunction in Eqn. (9) as the $\phi_0(p - Ft)$ in Eqn. (30), we can evaluate the position-space solution using Eqn. (8) to obtain

$$\begin{aligned} \psi(x, t) = & \left[e^{iFt(x_0 - Ft^2/6m)/\hbar} e^{i(p_0 + Ft)(x - x_0 - p_0 t/2m)/\hbar} \right] \left(\frac{1}{\sqrt{\sqrt{\pi}\alpha\hbar}(1 + it/t_0)} \right) \\ & \times e^{-(x - (x_0 + p_0 t/m + Ft^2/2m))^2 / 2(\alpha\hbar)^2 (1 + it/t_0)}. \end{aligned} \quad (35)$$

The corresponding probability density is given by

$$P(x, t) = \frac{1}{\sqrt{\pi}\beta_t} e^{-(x - \tilde{x}(t))^2 / \beta_t^2} \quad (36)$$

where

$$\tilde{x}(t) \equiv x_0 + \frac{p_0 t}{m} + \frac{Ft^2}{2m} \quad (37)$$

and

$$\langle x \rangle_t = \tilde{x}(t), \quad \langle x^2 \rangle_t = (\tilde{x}(t))^2 + \frac{\beta_t^2}{2}, \quad \text{and} \quad \Delta x_t = \frac{\beta_t}{\sqrt{2}} \quad (38)$$

so that this accelerating wave packet spreads in the same manner as the free-particle Gaussian example. The calculation of the kinetic energy density proceeds exactly as in Sec. II, with

$$\mathcal{T}(x, t) = \frac{1}{2m} \left((p_0 + Ft)^2 + \frac{2(p_0 + Ft)(x - \tilde{x}(t))}{\hbar\alpha^2} \frac{t/t_0}{(1 + t^2/t_0^2)} + \frac{(x - \tilde{x}(t))^2}{(\alpha^2\hbar)^2(1 + t^2/t_0^2)} \right) |\psi(x, t)|^2 \quad (39)$$

The corresponding (+) and (-) kinetic energies are then derived in the same way as before and are given by

$$T^{(\pm)}(t) = \frac{1}{2m} \left(\frac{1}{2} \right) \left((p_0 + Ft)^2 \pm \left(\frac{2(p_0 + Ft)}{\alpha\sqrt{\pi}} \right) \left(\frac{t/t_0}{\sqrt{1 + t^2/t_0^2}} \right) + \frac{1}{2\alpha^2} \right) \quad (40)$$

which is the same result as in Eqn. (19), with $p_0 \rightarrow p_0 + Ft$. This similarity in form implies that the maximum (minimum) values of $T^{(\pm)}(t)$ are once again given by Eqn. (22) (provided that $t/t_0 \gg 1$) which now occurs when $|p_0 + Ft| = \Delta p_0$. In this more dynamic situation, if p_0 and F have different signs (so that the motion includes one ‘back’ and one ‘forth’ component), this situation can occur twice during a single trajectory, with the roles of $R^{(+)}(t)$ and $R^{(-)}(t)$ changing between the ‘back’ and the ‘forth’ traversal.

IV. SIMPLE HARMONIC OSCILLATOR WAVE PACKETS

The third model system which is easily shown to exhibit time-dependent Gaussian wave packet solutions is also the most frequently studied of all classical and quantum mechanical examples, namely the simple harmonic oscillator, defined by the potential energy $V(x) = m\omega^2 x^2/2$. In this case, the initial value problem is perhaps most easily solved, especially for Gaussian wave packets, by propagator techniques [11] – [16]. In this approach, one writes

$$\psi(x, t) = \int_{-\infty}^{+\infty} dx' \psi(x', 0) K(x, x'; t, 0) \quad (41)$$

where the propagator can be derived in a variety of ways [16] and can be written in the form

$$K(x, x'; t, 0) = \sqrt{\frac{m\omega}{2\pi i\hbar \sin(\omega t)}} \exp \left[\frac{im\omega}{2\hbar \sin(\omega t)} ((x^2 + (x')^2) \cos(\omega t) - 2xx') \right]. \quad (42)$$

For the initial state wavefunction we will use position-space version of Eqn. (9), but for notational and visualization simplicity, we will specialize to the case of $x_0 = 0$, namely

$$\psi(x', 0) = \frac{1}{\sqrt{\beta\sqrt{\pi}}} e^{ip_0 x'/\hbar} e^{-(x')^2/2\beta^2} \quad (43)$$

where $\beta = \alpha\hbar$ and $\Delta x_0 = \beta/\sqrt{2}$. In this state, the expectation value of the energy is

$$\langle \hat{E} \rangle_t = \langle \hat{E} \rangle_0 = \frac{1}{2m} \left(p_0^2 + \frac{\hbar^2}{2\beta^2} \right) + \frac{m\omega^2\beta^2}{4} \quad (44)$$

The integral in Eqn. (41) can be done in closed form for the initial Gaussian in Eqn. (43) with the result

$$\psi(x, t) = \exp \left[\frac{im\omega x^2 \cos(\omega t)}{2\hbar \sin(\omega t)} \right] \frac{1}{\sqrt{A(t)}\sqrt{\pi}} \exp \left[-\frac{im\omega\beta}{2\hbar \sin(\omega t)} \frac{(x - x_s(t))^2}{A(t)} \right] \quad (45)$$

where

$$A(t) \equiv \beta \cos(\omega t) + i \left(\frac{\hbar}{m\omega\beta} \right) \sin(\omega t) \quad \text{and} \quad x_s(t) \equiv \frac{p_0 \sin(\omega t)}{m\omega}. \quad (46)$$

(We note that in the force-free limit, when $\omega \rightarrow 0$, one can show that this solution reduces to the free-particle form in Eqn. (12), with $x_0 = 0$, as expected.) The time-dependent probability density is given by

$$P(x, t) = |\psi(x, t)|^2 = \frac{1}{\sqrt{\pi}|A(t)|} e^{-(x-x_s(t))^2/|A(t)|^2} \quad (47)$$

where

$$|A(t)| = \sqrt{\beta^2 \cos^2(\omega t) + (\hbar/m\omega\beta)^2 \sin^2(\omega t)} \quad (48)$$

and

$$\langle x \rangle_t = x_s(t) \quad \text{and} \quad \Delta x_t = \frac{|A(t)|}{\sqrt{2}}. \quad (49)$$

So, while the expectation value of the wave packet oscillates in a way which mimics the classical result, the time-dependent spatial width of the packet changes in time, consistent with very general expectations for the oscillator case [17], [18]. This more general time-dependent Gaussian solution is described in several textbooks [7], [13] and special cases of it are often rediscovered [19], [20].

We note that in the special case of the minimum uncertainty wavepacket where

$$\beta^2 = \left(\frac{\hbar}{m\omega\beta} \right)^2 \quad \text{or} \quad \beta = \sqrt{\frac{\hbar}{m\omega}} \equiv \beta_0 \quad (50)$$

the time-dependent width of the Gaussian simplifies to

$$\Delta x_t = \frac{\beta_0}{\sqrt{2}} = \Delta x_0 \quad (51)$$

so the wave packet oscillates with no change in shape. This is the special result seen more standardly [21] – [27] in textbooks and pedagogical articles, and is similar to the coherent-state like solution discussed by Schrödinger [1] in a famous paper.

The time-dependent expectation value of the potential energy is easily found to be

$$\langle V(x) \rangle_t = \frac{1}{2} m \omega^2 \langle x^2 \rangle_t = \frac{1}{2m} \left(p_0^2 + \frac{\hbar^2}{2\beta^2} \right) \sin^2(\omega t) + \frac{m\omega^2 \beta^2 \cos^2(\omega t)}{4}. \quad (52)$$

The time-dependent (total) kinetic energy then follows directly from this equation combined with Eqn. (44) and is given by

$$T(t) = \frac{1}{2m} \langle p^2 \rangle_t = \frac{1}{2m} \left(p_0^2 + \frac{\hbar^2}{2\beta^2} \right) \cos^2(\omega t) + \frac{m\omega^2 \beta^2 \sin^2(\omega t)}{4}. \quad (53)$$

In order to determine the *distribution* of kinetic energy, however, we evaluate $\mathcal{T}(x, t)$ using

$$\frac{\partial \psi(x, t)}{\partial x} = \left(\frac{im\omega}{\hbar \sin(\omega t)} \right) \left(x \cos(\omega t) - \frac{\beta(x - x_s(t))}{A(t)} \right) \psi(x, t) \quad (54)$$

and we find that

$$T^{(\pm)}(t) = \frac{T(t)}{2} \pm \frac{p_0 \omega \sin(\omega t) \cos^2(\omega t)}{2\sqrt{\pi} |A(t)|} \left[\frac{\beta_0^4}{\beta^2} - \beta^2 \right]. \quad (55)$$

The asymmetry ($T^{(+)}(t) \neq T^{(-)}(t)$) in the kinetic energy distribution vanishes at half-integral multiples of the classical period $\tau \equiv 2\pi/\omega$, namely when $t = n\tau/2$, but also at the classical turning points, *i.e.*, at odd multiples of $\tau/4$. There is also no asymmetry in the case when $p_0 = 0$ and the wave packet expands and contracts uniformly in both the $+x$ and $-x$ directions. Finally, there is no asymmetry in the special case of the ‘fixed width’ Gaussian, when $\beta = \beta_0$, and this property can perhaps help explain some of the special features of that minimum-uncertainty state.

To better visualize the general result in Eqn. (55), we plot in Figs. 3 and 4 representations of both the wave function (modulus, real, and imaginary parts) as well as the probability ($P(x, t)$) and (scaled) kinetic energy ($S(x, t)$) distributions over the first quarter period. We note that for wave packets initially moving to the right ($p_0 > 0$) as shown here, narrow packets, *i.e.*, ones with $\beta < \beta_0$, typically have more kinetic energy in the ‘front’ half of the packet (Fig. 3, middle panels), while initially wider packets have the opposite behavior (Fig. 4) consistent with Eqn. (55).

While the time-dependence of $R^{(\pm)}(t)$ (defined in Eqn. (20)) is more varied than for the simpler, non-periodic, cases considered so far, as a specific example, we can examine the

distribution of kinetic energy at times such that

$$\cos(\omega T) = \sin(\omega T) = \frac{1}{\sqrt{2}} \quad \text{for instance, when} \quad T = \frac{\tau}{8}. \quad (56)$$

In that case we find

$$R^{(\pm)}(T) = \frac{1}{2} \pm \left(\frac{2}{\sqrt{\pi}} \right) \left(\frac{(p_0/m\omega)}{(2(p_0/m\omega)^2 + (\beta_0^4/\beta^2 + \beta^2))} \right) \left(\frac{(\beta_0^4/\beta^2) - \beta^2}{\sqrt{(\beta_0^4/\beta^2) + \beta^2}} \right) \quad (57)$$

This has extremal values of

$$R^{(\pm)}(T) = \frac{1}{2} \pm \frac{1}{\sqrt{2\pi}} \left[\frac{\beta_0^4/\beta^2 - \beta^2}{\beta_0^4/\beta^2 + \beta^2} \right] \quad (58)$$

when

$$p_0 = \sqrt{\frac{(\beta m \omega)^2}{2} + \frac{\hbar^2}{2\beta^2}} \quad (59)$$

which are obvious generalizations of Eqns. (22) and (23).

V. ‘INVERTED’ OSCILLATOR WAVE PACKETS FOR UNSTABLE EQUILIBRIUM

The final case we present for which time-dependent Gaussian wave packet solutions are easily obtained is a generalization of the harmonic oscillator which has been described as the ‘inverted oscillator’ [14] or the ‘unstable particle’ [28], corresponding to the classical motion of a particle at the top of potential hill, given by

$$\tilde{V}(x) \equiv -\frac{1}{2}m\tilde{\omega}^2x^2. \quad (60)$$

Many of the results obtained using propagator techniques can be easily carried over to this problem with the simple identifications

$$\omega \rightarrow i\tilde{\omega}, \quad \sin(\omega t) \rightarrow i \sinh(\tilde{\omega}t), \quad \text{and} \quad \cos(\omega t) \rightarrow \cosh(\tilde{\omega}t). \quad (61)$$

For example, the position-space probability density corresponding to the initial state in Eqn. (43) is given by

$$P(x, t) = |\psi(x, t)|^2 = \frac{1}{\sqrt{\pi}|B(t)|} \exp^{-(x-\tilde{x}_s(t))^2/|B(t)|^2} \quad (62)$$

where

$$|B(t)| = \sqrt{\beta^2 \cosh^2(\tilde{\omega}t) + (\hbar/m\tilde{\omega}\beta)^2 \sinh^2(\tilde{\omega}t)} \quad (63)$$

and

$$\langle x \rangle_t = \tilde{x}_s(t) = \frac{p_0 \sinh(\tilde{\omega}t)}{m\tilde{\omega}} \quad \text{and} \quad \Delta x_t = \frac{|B(t)|}{\sqrt{2}} \quad (64)$$

and the probability density exhibits a ‘runaway’ (exponential) behavior. In this case, the long time behavior of the kinetic energy fractions is dictated by the limits

$$\cosh(\tilde{\omega}t), \sinh(\tilde{\omega}t) \longrightarrow e^{\tilde{\omega}t}/2 \quad (65)$$

which gives

$$R^{(\pm)}(t \rightarrow \infty) = \frac{1}{2} \pm \left(\frac{2}{\sqrt{\pi}} \right) \left[\frac{(p_0/m\tilde{\omega})}{2(p_0/m\tilde{\omega})^2 + (\beta_0^4/\beta^2 + \beta^2)} \right] \sqrt{\beta_0^4/\beta^2 + \beta^2} \quad (66)$$

with the same extremal values as in Eqn. (22), when p_0 satisfies the equivalent of Eqn. (59) with $\omega \rightarrow \tilde{\omega}$.

VI. CONCLUSIONS AND DISCUSSION

In this note we have provided a detailed analysis of Gaussian wave packet solutions of the Schrödinger equation in several model systems, helping to elucidate some of the qualitative aspects of wave packet time-development and spreading often seen in standard visualizations, and their relationship to the distribution of kinetic energy. We have focused on closed-form analytic results, all of which have been obtainable due to the special nature of the integrals which arise for Gaussian wave packets. An obvious and interesting extension would be to extend these results to free particle wave packets for arbitrary non-Gaussian initial momentum distributions, performing the required integrals in Eqn. (8) numerically to see just how general the results in Eqns. (22) and (23) are. For example, are there other initial wave packets and initial conditions for which the kinetic energy can be even more localized than the 90%/10% fraction seen here for Gaussians? Another straightforward generalization is to consider two-dimensional extensions of all four systems discussed here (then visualized as functions of both x and y) where closed form expressions are also possible, as well as the related case of the charged particle (confined to a plane) subject to a uniform magnetic field.

Other studies of dynamical wave packet propagation have discussed aspects of the time-development of $\psi(x, t)$ which arise from effects related to the differing behavior of various momentum-components. Examples have included discussions of the average speed of wave packet components which are transmitted or reflected from a rectangular barrier [29] (due to the energy dependence of probabilities of transmission and reflection) as well as the time-dependent shape of $|\phi(p, t)|^2$ for a wave packet hitting an infinite wall [30] or similar ‘bouncing’ systems [31]. The consideration of the distribution of kinetic energy distribution in many other such time-dependent wave packet solutions might prove useful in understanding their behavior. One such example certainly would be Gaussian-like wave packet solutions in the infinite square well, where additional interesting features, such as exact wave packet revivals, are present.

Gaussian solutions such as those considered here can find use as examples of model systems in discussing other theoretical constructs, such as the Wigner quasi-probability distribution [32] - [42]. In that case, one defines $P_W(x, p; t)$ via

$$P_W(x, p; t) \equiv \frac{1}{\pi\hbar} \int_{-\infty}^{+\infty} \psi^*(x + y, t) \psi(x - y, t) e^{2ipy/\hbar} dy \quad (67)$$

$$= \frac{1}{\pi\hbar} \int_{-\infty}^{+\infty} \phi^*(p + q, t) \phi(p - q, t) e^{-2ixq/\hbar} dq \quad (68)$$

which can then be evaluated explicitly in closed form, in either position- or momentum-space, for all of the solutions discussed above. In an accompanying paper [43] we study the same four examples considered here, in yet a different context.

-
- [1] E. Schrödinger, *Der stetige Übergang von der Mikro- zur Makromechanik* Naturwissenschaften **14** 664-666 (1926) translated and reprinted as *The continuous transition from micro- to macro mechanics*, in *Collected papers on wave mechanics* (Chelsea Publishing, New York, 1982) pp 41-44.
- [2] E. H. Kennard, *The quantum mechanics of an electron or other particle*, J. Franklin Institute **207**, 47-78 (1929); see also *Zur quantenmechanik einfacher Bewegungstypen*, Z. Phys. **44**, 326-352 (1927).
- [3] C. G. Darwin, *Free motion in the wave mechanics*, Proc. Roy. Soc (London) **A117**, 258-293 (1928).
- [4] L. de Broglie, *Einführung in die Wellenmechanik* (Akad. Verlag. Leipzig, 1929)
- [5] E. C. Kemble, *The fundamental principles of quantum mechanics with elementary applications*, (McGraw-Hill, New York, 1937) pp 35-41.
- [6] S. Dushman, *The elements of quantum mechanics*, (Wiley, New York, 1938) pp 405-407.
- [7] V. Rojansky, *Introductory Quantum Mechanics* (Prentice Hall, New York, 1938) pp 69-70.
- [8] J. R. Hiller, I. D. Johnston, and D. F. Styer, *Quantum Mechanics Simulations: The Consortium for Upper-Level Physics Software* (Wiley, New York, 1995).
- [9] B. Thaller, *Visual Quantum Mechanics: Selected Topics with Computer-Generated Animations of Quantum-Mechanical Phenomena* (Springer-Verlag, New York, 2000).
- [10] M. Belloni and W. Christian, *Physlets for quantum mechanics*, Comp. Sci. Eng. **5**, 90-97 (2003).
- [11] R. P. Feynman, *Space-time approach to non-relativistic quantum mechanics*, Rev. Mod. Phys. **20**, 367-387 1948.
- [12] R. P. Feynman and A. R. Hibbs, *Quantum mechanics and path integrals* (McGraw-Hill, New York, 1965).
- [13] D. S. Saxon, *Elementary Quantum Mechanics* (McGraw-Hill, New York, 1968) pp 144-147.
- [14] P. Nardone, *Heisenberg picture in quantum mechanics and linear evolutionary systems*, Am. J. Phys. **61**, 232-237 (1993).
- [15] S. M. Cohen, *Path integral for the quantum harmonic oscillator using elementary methods*, Am. J. Phys. **66**, 537-540 (1998).

- [16] B. R. Holstein, *The harmonic oscillator propagator*, Am. J. Phys. **66**, 583-589 (1998).
- [17] K. Gottfried, *Quantum Mechanics: Volume I Fundamentals* (Benjamin, New York, 1966) pp 260-264.
- [18] D. F. Styer, *The motion of wave packets through their expectation values and uncertainties*, Am. J. Phys. **58**, 742-744 (1990).
- [19] A. S. de Castro and N. C. da Cruz, *A pulsating Gaussian wave packet*, Eur. J. Phys. **20**, L19-L20 (1999).
- [20] W. Waldenström and Razi K. Naqvi, *A neglected aspect of the pulsating Gaussian wave packet*, Eur. J. Phys. **20**, L41-L43 (1999).
- [21] L. I. Schiffer, *Quantum Mechanics* (First Edition) (McGraw Hill, New York, 1949) pp 67-69.
- [22] D. Bohm, *Quantum Theory* (Prentice-Hall, Englewood Cliffs, 1951) pp 306-309.
- [23] P. Fong, *Elementary Quantum Mechanics* (Addison-Wesley, Reading, 1962) pp 88-91.
- [24] A. Messiah, *Quantum Mechanics: Volume I* (North-Holland, Amsterdam, 1961) pp 446-447.
- [25] D. ter Haar, *Selected Problems in Quantum Mechanics* (Academic Press, New York, 1964) pp 14, 143-145.
- [26] C. Cohen-Tannoudji, B. Diu, and F. Laloë, *Quantum Mechanics: Volume I* (Wiley, New York, 1977) pp 572-573.
- [27] S. Howard and S. K. Roy, *Minimum uncertainty states and their time evolution*, Am. J. Phys. **53**, 538-542 (1985).
- [28] R. W. Robinett, *Quantum Mechanics: Classical Results, Modern Systems, and Visualized Examples* (Oxford University Press, New York, 1997) pp 208-209, 213-214.
- [29] M. H. Bramhall and B. M. Casper, *Reflections on a wave packet approach to quantum mechanical barrier penetration*, Am. J. Phys. **38**, 1136-1145 (1970).
- [30] M. A. Doncheski and R. W. Robinett, *Anatomy of a 'quantum bounce'*, Eur. J. Phys **20**, 29-37 (1999).
- [31] L. de la Torre and F. Gori, *The bouncing bob: quasi-classical states*, Eur. J. Phys. **24**, 253-259 (2003).
- [32] E. Wigner, *On the quantum correction for thermodynamic equilibrium*, Phys. Rev. **40**, 749-759 (1932).
- [33] V. I. Tatarskii, *The Wigner representation of quantum mechanics*, Sov. Phys. Usp. **26**, 311-327 (1983).

- [34] N. L. Balaczs and B. K. Jennings, *Wigner's function and other distribution functions in mock phase space*, Phys. Rep. **105**, 347-391 (1984).
- [35] P. Carruthers and F. Zachariasen, *Quantum collision theory with phase-space distributions*, Rev. Mod. Phys. **55**, 245-285 (1983).
- [36] M. Hillery, R. F. O'Connell, M. O. Scully, and E. P. Wigner, *Distribution functions in physics: Fundamentals*, Phys. Rep. **106**, 121-167 (1984).
- [37] J. Bertrand and P. Bertrand, *A tomographic approach to Wigner's function*, Found. Phys. **17**, 397-405 (1987).
- [38] Y. S. Kim and E. P. Wigner, *Canonical transformations in quantum mechanics*, Am. J. Phys. **58**, 439-448 (1990).
- [39] Y. S. Kim and M. E. Noz, *Phase space picture of quantum mechanics: Group theoretical approach*, Lecture Notes in Physics Series, Vol. 40 (World Scientific, Singapore, 1990)
- [40] H.-W. Lee, *Theory and application of the quantum phase-space distribution functions*, Phys. Rep. **259**, 147-211 (1995).
- [41] A. M. Ozorio de Almeida, *The Weyl representation in classical and quantum mechanics*, Phys. Rep. **296**, 265-342 (1998)
- [42] M. Belloni, M. Doncheski, and R. W. Robinett, *Wigner quasi-probability distribution for the infinite square well: energy eigenstates and time-dependent wave packets*; e-Print arXiv: quant-ph/0312086.
- [43] R. W. Robinett and L. C. Bassett, *Analytic results for Gaussian wave packets in four model systems: II. Autocorrelation functions*, submitted to Found. Phys.

Figure Captions

- Fig. 1. Time-development of a free-particle Gaussian wave packet, illustrating the modulus ($|\psi(x, t)|$, solid), the real ($Re(\psi(x, t))$, dotted) and imaginary ($Im(\psi(x, t))$, dashed) parts, as functions of time.
- Fig. 2. The figures in the left column show the modulus (solid), and the real (dotted) and imaginary (dashed) parts of Gaussian wave packets at long times ($t = 10t_0$) plotted versus $x_0 + p_0t/m$, illustrating the large fraction of kinetic energy (note the pattern of ‘wiggleness’) in the front of the wave for the $p_0 = \Delta p_0$ case, as in Eqn. (22). In the right column, we plot the probability density ($|\psi(x, t)|^2$, solid) and the (scaled) kinetic energy density ($S(x, t) = \mathcal{T}(x, t)/T(t)$, dashed) from Eqn. (24).
- Fig. 3. The figures in the top row show the modulus (solid), and the real (dotted) and imaginary (dashed) parts of Gaussian wave packet solutions of the harmonic oscillator corresponding to $x_0 = 0$ and $p_0 > 0$ with $\beta = \beta_0/2 < \beta_0$. Times over the first quarter period are shown. In the bottom row, we plot the probability density ($|\psi(x, t)|^2$, solid) and the (scaled) kinetic energy density ($S(x, t) = \mathcal{T}(x, t)/T(t)$, dashed) from Eqn. (24) at the corresponding times.
- Fig. 4. Same as Fig. 3, but for an initial Gaussian wave packet solution of the harmonic oscillator with $\beta = 2\beta_0 > \beta_0$.

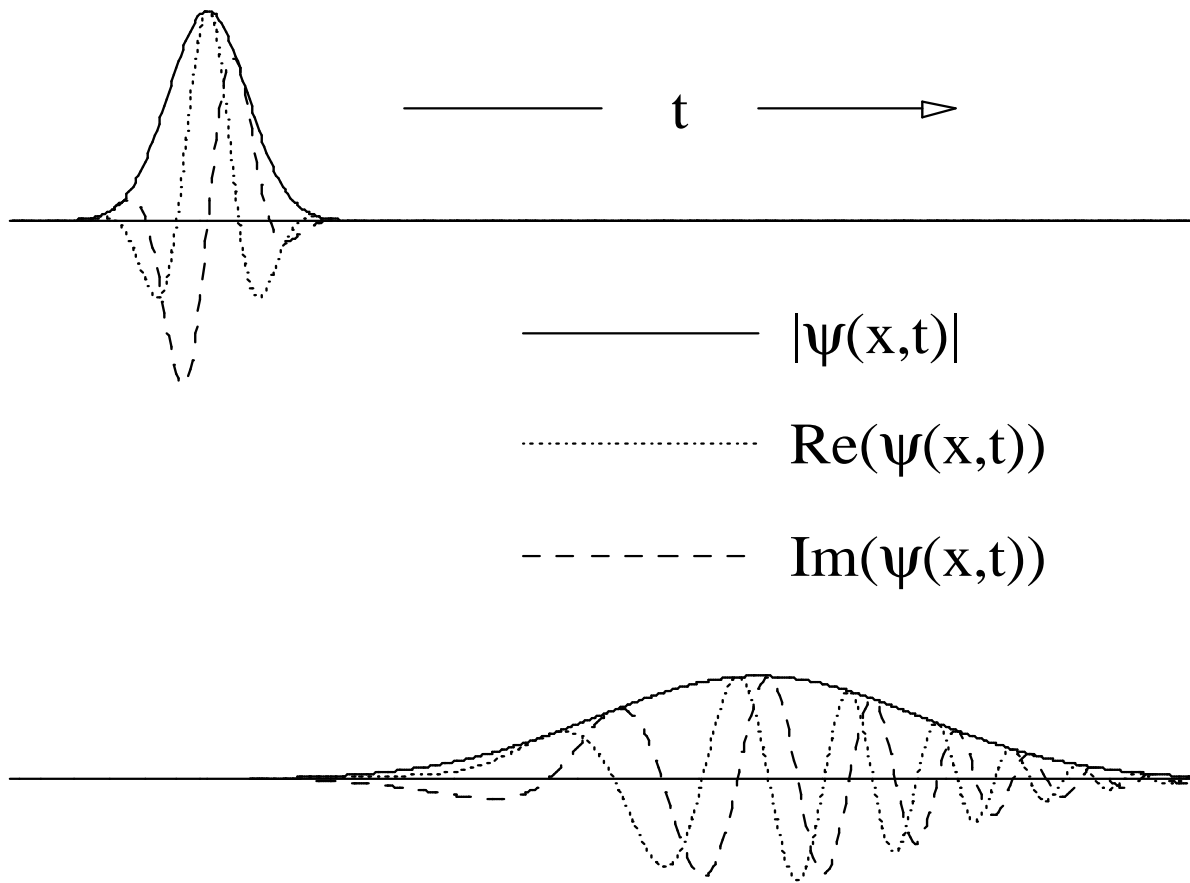
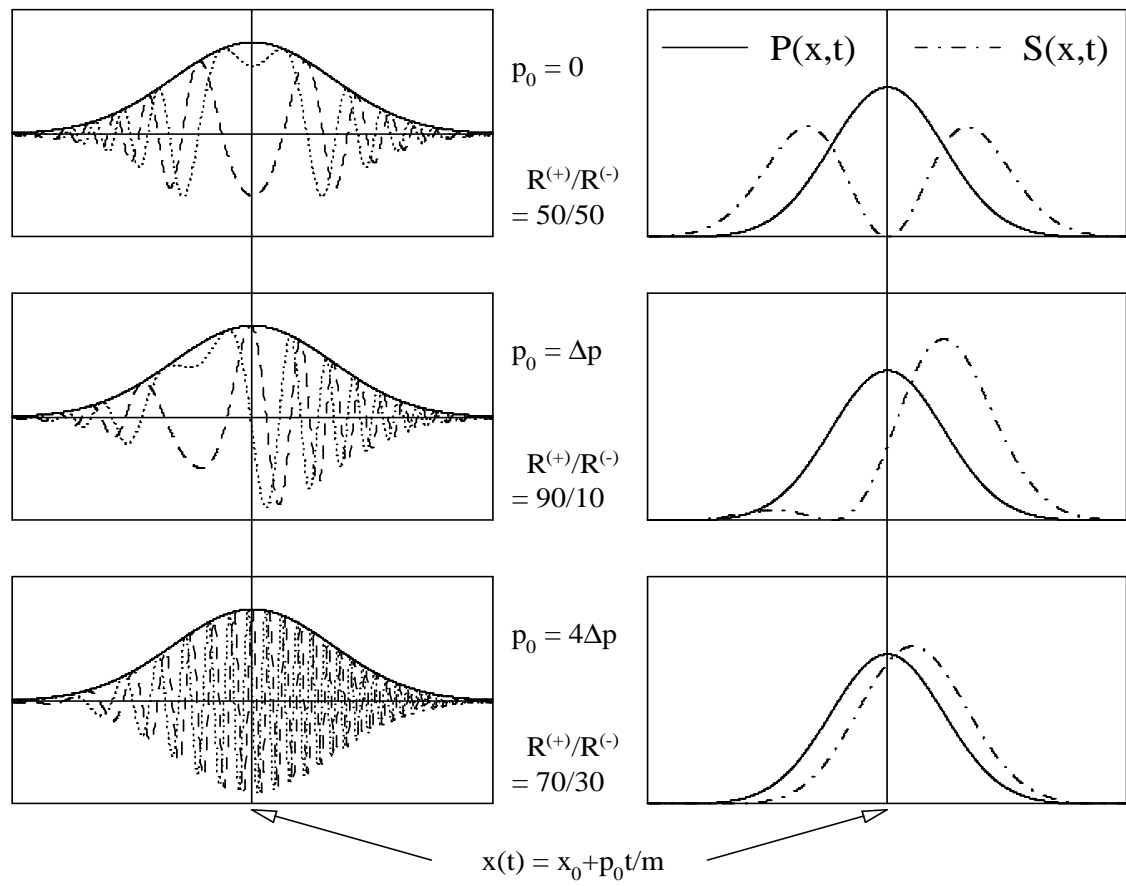


FIG. 1:

FIG. 2:



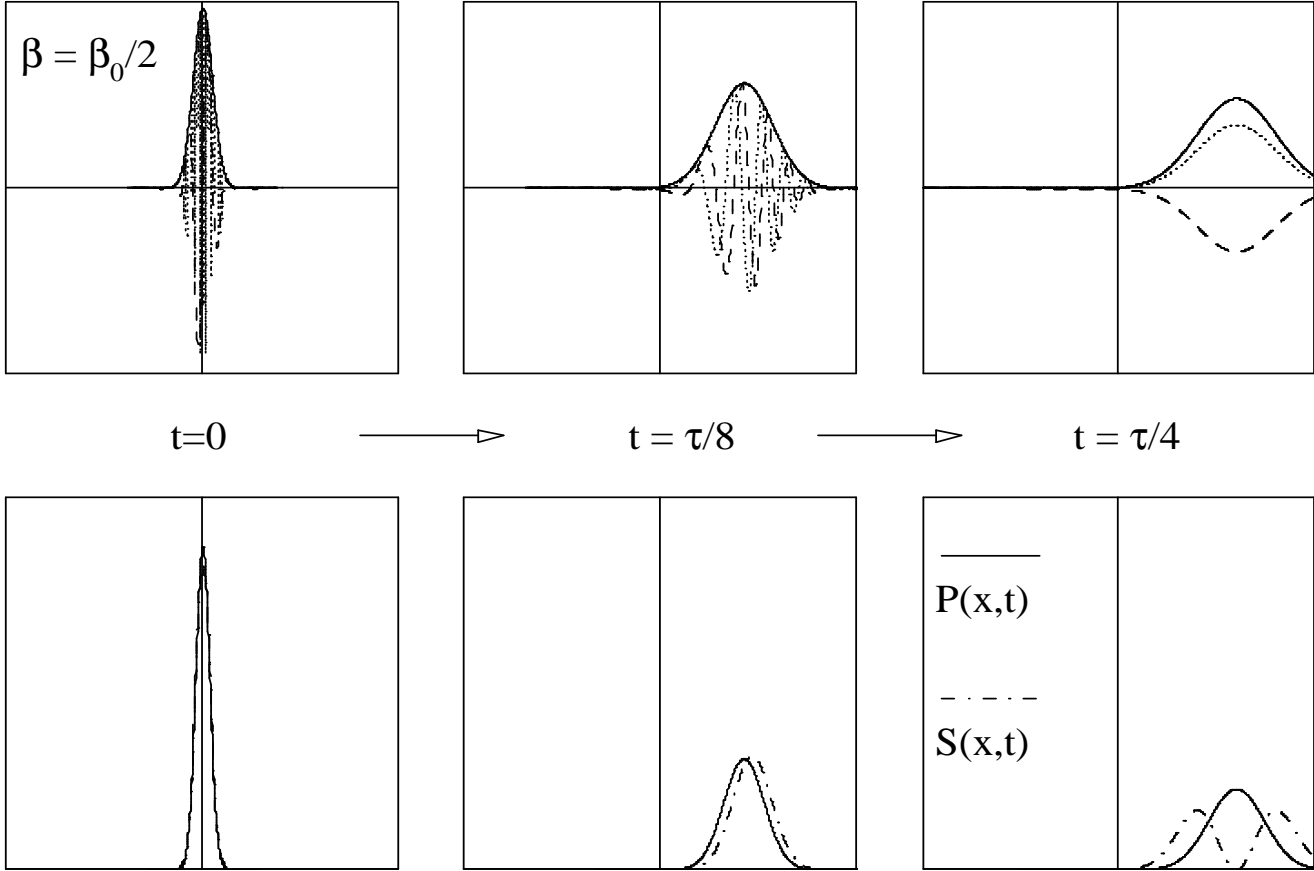


FIG. 3:

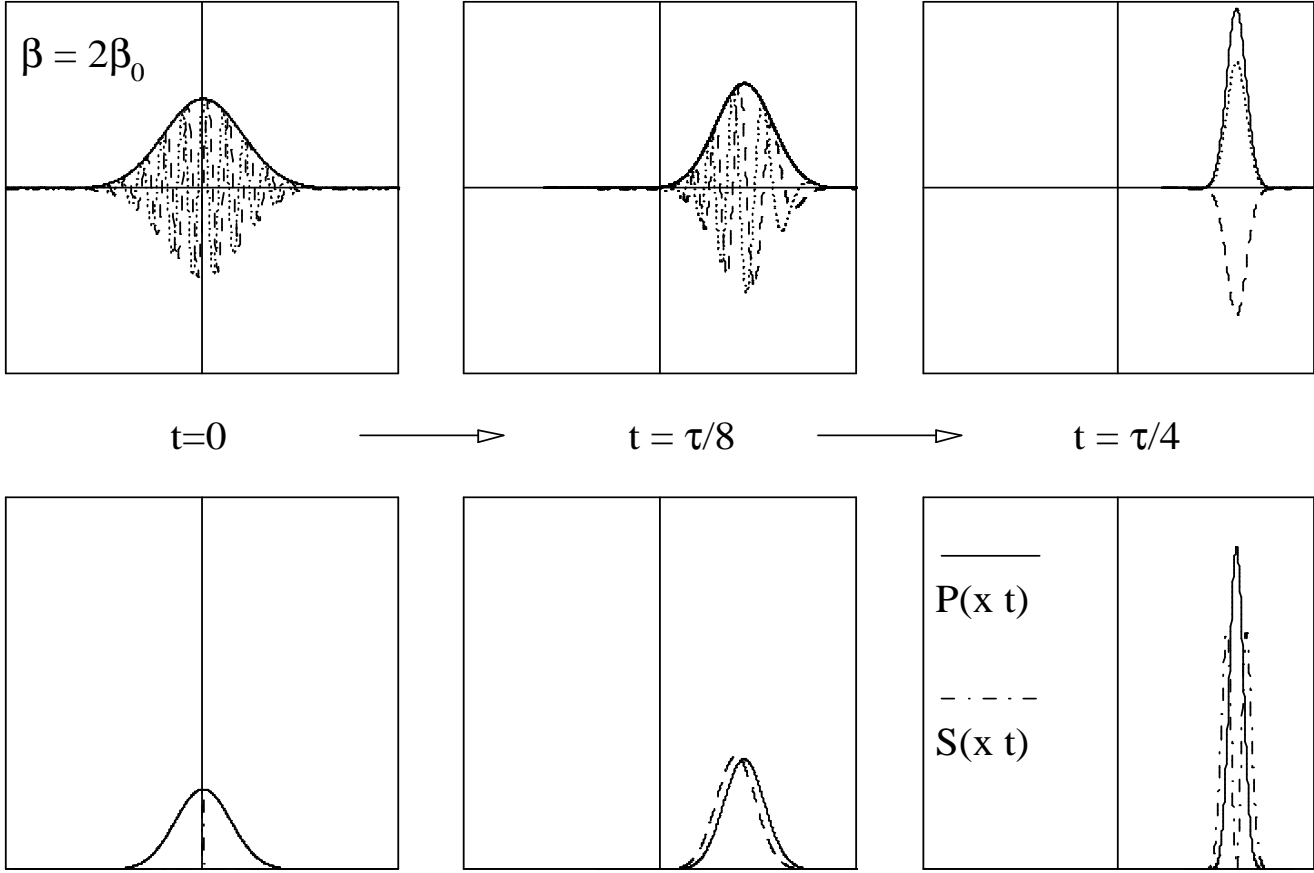


FIG. 4: